ELSEVIER

Journal of Biomechanics 34 (2001) 1491–1500

JOURNAL OF BIOMECHANICS

www.elsevier.com/locate/jbiomech
www.JBiomech.com

A 3-D dynamic model of human finger for studying free movements

J.L. Sancho-Bru[a,*], A. Pérez-González[a], M. Vergara-Monedero[a], D. Giurintano[b]

[a] *Departament de Tecnologia, Universitat Jaume I, Campus de Riu Sec, 12071 Castellò, Spain*
[b] *Paul Brand Biomechanics Laboratory, National Hansen's Disease Center, 1770 Physicians Park Drive, Baton Rouge, LA, USA*

Accepted 18 February 2001

Abstract

The purpose of this work is to develop a 3D inverse dynamic model of the human finger for estimating the muscular forces involved during free finger movements. A review of the existing 3D models of the fingers is presented, and an alternative one is proposed. The validity of the model has been proved by means of two simulations: free flexion–extension motion of all joints, and free metacarpophalangeal (MCP) adduction motion. The simulation shows the need for a dynamic model including inertial effects when studying fast movements and the relevance of modelling passive forces generated by the structures studying free movements, such as the force exerted by the muscles when they are stretched and the passive action of the ligaments over the MCP joint in order to reproduce the muscular force pattern during the simulation of the free MCP abduction–adduction movements. © 2001 Elsevier Science Ltd. All rights reserved.

Keywords: Biomechanics; Finger modelling; Hand modelling; MCP collateral ligament; Free movement

1. Introduction

Biomechanical models of the human hand are of great importance in the biomedical and medical ergonomic fields. Different aspects of hand function have been investigated by various researchers. To date, no work analysing the features a model requires in order to study the behaviour of the finger during free flexion–extension and abduction–adduction movements has been published. Most of the models in the literature are 2D models, allowing the study of the finger behaviour in the sagittal plane, so that only flexion–extension movements of the fingers can be analysed. Only a few 3D models have been developed (Chao et al., 1976; Chao and An, 1978; Casolo and Lorenzi, 1994; Biryukova and Yourovskaya, 1994; Mansour et al., 1994; Esteki and Mansour, 1997; Valero-Cuevas et al., 1998), which would allow the study of metacarpophalangeal (MCP) joint movements. Only the models of Biryukova and Yourovskaya (1994) and Esteki and Mansour (1997) allowed the study of dynamic actions. The passive action of muscles and the dependence of muscle force on its length and activation level were considered only in the static model of Mansour et al. (1994). The contraction velocity dependence was also included in the latter dynamic model of Esteki and Mansour (1997). None of the models included the ligaments, although the importance of considering the passive moment at the joints for the hand of tetraplegic patients for studying the unloaded finger was emphasised in Mansour et al. (1994). In this work, the passive moment at each joint was introduced from a series of measurements made rotating manually one joint of the finger and keeping the other two fixed in the neutral position. The work did not take into account that the passive moment measured lumped together the action of the ligamentous structure and the passive action of muscles. Furthermore, the model for the passive moments did not consider the coupling effect of flexion–extension and abduction–adduction motion on the MCP joint.

In this paper, a 3D inverse dynamic model of the index finger for estimating the muscular forces involved during free finger movements is introduced. The model is used to examine the need of modelling the passive forces generated by muscles and MCP ligaments when analysing these movements as well as the need of considering the inertial effects when studying fast movements. The inverse dynamic model proposed considers the muscle force dependence on length,

*Corresponding author. Tel.: 34-964-72-81-27; fax: 34-964-72-81-06.
E-mail address: sancho@tec.uji.es (J.L. Sancho-Bru).

PII: S0021-9290(01)00106-3

Nomenclature

2D	Two-dimensional
3D	Three-dimensional
CE	Contractile element
DIP	Distal interphalangeal
DOF	Degrees of freedom
EDC	Extensor digitorum communis
EI	Extensor indicis
EMG	Electromyographic
FDP	Flexor digitorum profundus
FDS	Flexor digitorum superficialis
IP	Interphalangeal
LU	Lumbrical
MCP	Metacarpophalangeal
PCSA	Physiological cross-sectional area
PEE	Parallel elastic element
PIP	Proximal interphalangeal
RI	Radial interosseous
SEE	Series elastic element
UI	Ulnar interosseous

contraction velocity and activation level. The action of collateral ligaments over the MCP joint is considered, taking into account the coupling effect of flexion–extension and abduction–adduction motions. In order to solve the indeterminate problem, a physiologically based optimisation criterion is used.

2. Materials and methods

A 3D dynamic model of the index finger is proposed and its validity to estimate the muscle force patterns during free motion is investigated by means of two simulations: free flexion–extension motion of all joints and free MCP adduction motion.

2.1. Model description

2.1.1. Skeletal segments

The finger has been considered as an open chain of rigid bodies (three phalanxes and the metacarpal) connected through different joints which characterise the kinematic behaviour of the chain. Segments have been represented by cylinders with masses assumed to be equal to the masses of corresponding bones plus all adjoining soft tissues. Segment masses and principal moments of inertia have been computed based on the segment volume, using a density of 1.1 g/cm^3 (Esteki and Mansour, 1997). Possible variations of segment inertial characteristics because of muscle contractions are neglected.

2.1.2. Kinematic constraints

Joint surfaces together with ligaments create the kinematic constraints between consecutive segments.

Distal interphalangeal (DIP) and proximal interphalangeal (PIP) joints connect distal to medial phalanx and medial to proximal phalanx, respectively. The shape of the articular surfaces and the arrangement of the connecting structures facilitate sagittal flexion–extension, while lateral movements and rotation are prevented (Dubousset, 1981). Therefore, they have been modelled as hinge joints capable of only flexion and extension. The insertion of the collateral ligaments on the proximal segment of the joint corresponds to the flexion–extension axis (Dubousset, 1981). They do not develop any flexion–extension moment over the joint; therefore, they do not need to be modelled.

The proximal phalanx is connected to the metacarpal by the MCP joint. Its configuration facilitates flexion–extension and lateral deviation movements (Dubousset, 1981). The joint is reinforced by the collateral ligaments, which prevent pronation and restrain the amplitude of lateral deviations. Therefore, it has been modelled as a universal joint capable only of flexion–extension and abduction–adduction. The proximal insertion of the lateral ligament on the metacarpal head remains dorsal to the centre of the articular curvature. (Fig. 1), so that collateral ligaments are lax in extension, but they become taut in flexion, decreasing significantly the range of lateral movement (Dubousset, 1981; Craig, 1992; Kapandji, 1998). Tension on the radial and ulnar ligaments increases with adduction and abduction of the MCP joint, respectively. The ligamentous forces are the only resistance the intrinsic muscles have to counteract during free abduction–adduction movements of the joint (Kapandji, 1998). Furthermore, the line of action of the ligaments remains dorsal to the flexion–extension axis of the joint (Craig, 1992), developing an extension moment over the joint, in addition to the abduction–adduction moment. Therefore, the collateral ligaments of the MCP joint have to be considered when developing a 3D model of the human finger.

Both ulnar and radial ligaments over the MCP joint have been considered. A unique fibre for each ligament

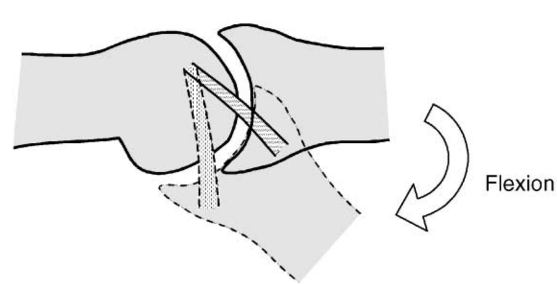

Fig. 1. Sketch of the collateral ligament over the MCP joint, showing how it becomes taut with flexion.

has been considered, joining two points representing the insertions into the bones. One point is fixed with respect to the metacarpal, and the other one with respect to the proximal phalanx. No interaction between bone and ligament has been considered, therefore, the ligament path is a straight line between the insertion points. Its non-linear behaviour has been taken into account considering a quadratic relationship between the force developed by the ligament (F_{lig}) and its elongation (Mommersteeg et al., 1996)

$$F_{lig} = K\left(L_{lig} - L_{lig,o}\right)^2, \quad (1)$$

where K is the characteristic constant of the ligament, L_{lig} the length of the fibre representing the ligament, and $L_{lig,o}$ the unstrained length of the ligament.

The data for the location and orientation of the rotation axes have been taken from An and Cooney (1991). The data for the ligament insertion points have been obtained from the geometric model presented in Youm et al. (1978), and the stiffness constant has been estimated to be 750 N/cm^2 from Minami et al. (1985).

2.1.3. Muscles

Muscles and tendons control the movement of the skeletal chain. Muscles are elements capable of generating force from the contraction of their fibres, but they also develop a passive force when they are stretched from their resting length. Musculotendon action has been modelled using a Hill's model (Fig. 2). The model considers three elements: a contractile element (CE), which is the basic component that generates force, a parallel elastic element (PEE), which is responsible of the passive force generated by the muscle when it is stretched, and a series elastic element (SEE), the muscle tendon unit.

The force that a muscle can exert depends on the actual muscle length and contraction velocity. It is widely accepted (An et al., 1991) that the maximum force a muscle can exert in optimal conditions, is proportional to its PCSA

$$F_{max} = \mathrm{PCSA} \times S_{max}, \quad (2)$$

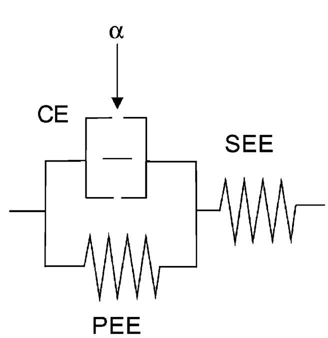

Fig. 2. Hill's three component model for the muscles.

where S_{max} is the maximum stress the muscle can bear, which has been considered the same for each muscle (An et al., 1991).

The strain of tendons is insignificant for the magnitude of forces developed by the muscles. Under this consideration, the SEE has been considered to be inextensible, so that the force the muscle exerts (F) can be written as

$$F = F_{max}(F_{CE} + F_{PEE}), \quad (3)$$

where F_{CE} and F_{PEE} are the normalised forces delivered by the CE and PEE, respectively. The force exerted by the muscle can be decomposed into an active force and a passive force corresponding to the forces delivered by the CE and PEE, respectively.

The force delivered by the CE is related to the muscle architecture and is a function of the muscle length l_{CE}, the contraction velocity v_{CE}, and the muscle activation level α (from 0 to 1), which is controlled by the central nervous system (Kaufman et al., 1991).

$$F_{CE} = \alpha \cdot F_l(l_{CE}) \cdot F_v(v_{CE}), \quad (4)$$

where F_l and F_v are the non-dimensional force–length and force–velocity relationships.

A characteristic bell-shaped curve exists between force and length of the muscle. To model this dependence, the expression proposed by Kaufman et al. (1991) has been used

$$F_l(\varepsilon, i_a) = \mathrm{e}^{-\left[\frac{(\varepsilon+1)^{0.96343\left(1-\frac{1}{i_a}\right)}-1.0}{0.35327(1-i_a)}\right]^2} \quad \text{for } i_a < 1, \quad (5a)$$

$$F_l(\varepsilon, i_a) = \mathrm{e}^{-[2.727277 \cdot \ln(\varepsilon+1)]^2} \quad \text{for } i_a = 1, \quad (5b)$$

where i_a is the muscle architecture index, defined as the ratio between the muscle fibre length and the muscle belly length, and ε is the muscle strain

$$\varepsilon = \frac{l - l_0}{l_0}, \quad (6)$$

where l is the actual muscle length and l_0 the muscle length for the optimal conditions (when the muscle can exert the maximum isometric force).

The force a muscle can exert decreases when the contraction velocity of the muscle fibres increases. To model this dependence the expression proposed by Hatze (1981) has been used

$$F_v(\dot{\eta}) = \frac{0.1433}{0.1074 + \mathrm{e}^{-1.409 \sin h(3.2\dot{\eta}+1.6)}}, \quad (7)$$

where $\dot{\eta}$ is the normalised contractile element velocity

$$\dot{\eta} = \frac{\dot{\varepsilon}}{\dot{\varepsilon}_{max}}, \quad (8)$$

where $\dot{\varepsilon}$ is the lengthening velocity of the muscle, and $\dot{\varepsilon}_{max}$ its maximal value.

The force generated by the PEE is a function only of its length. An exponential relationship has been considered in this case (Lee and Rim, 1990; Kaufman et al., 1991)

$$F_{\mathrm{PEE}} = b_1 \mathrm{e}^{b_2 \varepsilon} - b_1, \tag{9}$$

where b_1 and b_2 are muscle dependent constants.

The previous equations describe the model used to represent the behaviour of the index finger muscles. The index finger is controlled by seven muscles: radial interosseous (RI), ulnar interosseous (UI), lumbrical (LU), flexor digitorum profundus (FDP), flexor digitorum superficialis (FDS), extensor digitorum communis (EDC) and extensor indicis (EI). All these muscles have been considered, but both extrinsic extensors (EDC and EI) have been modelled as a unique entity. PCSA data for all muscles have been taken from Valero-Cuevas et al. (1998), while the muscle stress limit ($S_{\max}$) has been obtained from Zajac (1989). Fibre and muscle lengths and the constants b_1, b_2 have been taken from Lee and Rim (1990). The muscle maximal lengthening velocity ($\dot{\varepsilon}_{\max}$) has been taken to be $2.5\,\mathrm{s}^{-1}$ (Kaufman et al., 1991).

2.1.4. Tendons and tendon excursions

Most of the muscles do not act directly over the bones, but transmit the force to the tendons, which finally insert into the bones. To model the tendon action crossing the joints, straight lines connecting two points have been considered, one fixed with respect to the proximal bone and the other one with respect to the distal bone (Fig. 3a). This approximation has been found to be close enough to the behaviour of all tendons with the exception of extensors, for which Landsmeer's model I has been considered (Fig. 3b).

Hand tendons split along their path and present connections of other tendons. This is specially true for the extensor apparatus. The model's representation of the extensor mechanism, with its connections and the contribution of UI, LU and EDC + EI muscles, are depicted in Fig. 4. Appropriate force balances have been considered in the connecting points of this deformable tendon net. Straight lines between the connecting points of the net have been considered. All the tendon actions over each joint that have been considered in the model are listed in Table 1.

The muscle force–length and force–velocity relationships presented before require the calculation of the lengthening of the muscles from l_0 as a function of time. Having considered the tendons inextensible, the muscle lengthening coincides with the tendon excursion. For the FDP, FDS and RI, that do not present connections with other tendons, the excursion is simply the sum of their excursions around each joint. To calculate the tendon excursions at each joint, the same points that define the tendon action over the joint have been used. The

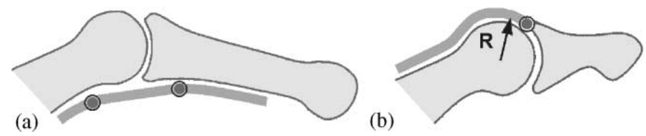

Fig. 3. Models for the tendons crossing the joints: (a) Straight lines; (b) Landsmeer's model I.

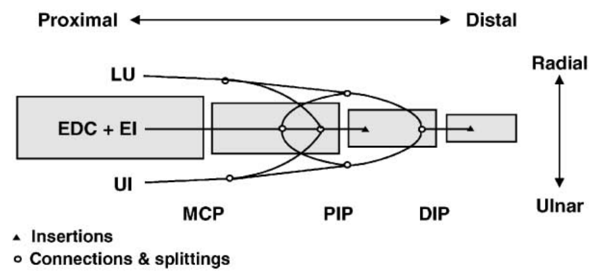

Fig. 4. Sketch of the extensor mechanism. Dorsal view.

Table 1
Tendon actions over each joint considered in the model

Joint	Tendons and muscles
DIP	Terminal extensor FDP
PIP	Extensor slip Radial band Ulnar band FDP FDS
MCP	RI UI LU FDP FDS EDC + EI

excursion for the FDP according to the lengths l_i shown in Fig. 5a is given by

$$\text{excursion (FDP)} = (l_1 + l_2 + l_3)_{\text{posture}} - (l_1 + l_2 + l_3)_{\text{reference}}. \tag{10}$$

The EDC + EI tendon presents a trifurcation over the proximal phalanx and two insertions, one into the base of the medial phalanx and the other one into the distal phalanx (Fig. 5a). To calculate the excursion, the case of the unloaded finger has been considered, so that the central band of the trifurcation (the extensor slip) is always taut. Therefore, the EDC + EI tendon excursion is the sum of the extensor slip excursion around the PIP joint and the EDC + EI tendon excursion around the MCP joint. According to Fig. 5a, the EDC tendon excursion can be expressed as

$$\text{excursion (EDC)} = (l_4 + l_5)_{\text{posture}} - (l_4 + l_5)_{\text{reference}}. \tag{11}$$

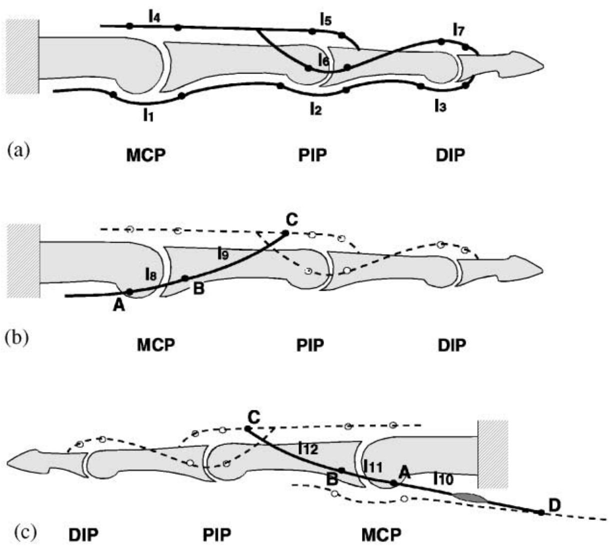

Fig. 5. Sketch of different tendons over the index finger: (a) FDP and EDC (medial view); (b) UI (medial view); (c) LU (lateral view).

UI tendon inserts into the extensor mechanism. To calculate the excursion a floating point C not fixed to any of the rigid bodies has been considered (Fig. 5b). Point C is defined so that the distance over the extensor slip path to its insertion remains constant. According to Fig. 5b, the UI tendon excursion is given by

$$\text{excursion (UI)} = (l_8 + l_9)_{\text{posture}} - (l_8 + l_9)_{\text{reference}}. \qquad (12)$$

LU muscle presents a similar configuration, but it inserts into the FDP tendon (Fig. 5c). A floating point D representing the origin of LU on the FDP tendon has been considered. According to Fig. 5c, the LU tendon excursion can be expressed as

$$\begin{aligned}\text{excursion (LU)} &= (l_{10} + l_{11} + l_{12})_{\text{posture}} \\ &\quad - (l_{10} + l_{11} + l_{12})_{\text{reference}}. \qquad (13)\end{aligned}$$

To calculate the length of the tendon path crossing each joint (l_i), straight lines connecting the points have been considered, except for the extensor tendons, for which a circular path has been considered.

2.1.5. Resolution

The finger has been considered as an open chain of rigid bodies with four DOF: flexion–extension of DIP, PIP and MCP joints and abduction–adduction of MCP joint. The passive action of the ligaments over MCP joint has been considered, as well as the passive and active actions of the musculotendon units. The posture as a function of time (angles and angular velocities and accelerations of all joints) are input to the model. The problem to be solved is to find the muscle activation levels required to produce the given motion. It is, therefore, an inverse dynamic problem.

The dynamic equations of the open chain of rigid bodies have been derived using the Lagrange method (García de Jalón and Bayo, 1994). For a system with m generalised co-ordinates q_k, this equation is expressed as

$$\frac{d}{dt}\frac{\partial L}{\partial \dot{q}_k} - \frac{\partial L}{\partial q_k} = Q_k^{nc} \quad k = 1, \ldots, m, \qquad (14)$$

where L is the Lagrangian function and Q_k^{nc} are the generalised non-conservative forces. The generalised coordinates have been considered to be coincident with the DOF of the system ($m = 4$): flexion of DIP, PIP and MCP joints and abduction of MCP joint.

Eq. (14) together with the force balances of the tendon nets lead to an indeterminate problem. There are 12 equations (four) corresponding to the DOF considered and eight to force balances in the tendon net) and 18 unknowns (six muscle forces and 12 branch forces of the tendon net).

There is not a unique combination of muscular efforts that satisfy the dynamic equilibrium constraints. To solve the problem, a criterion chosen by the central nervous system to determine the control of muscle action must be introduced. In this case, the endurance is maximised. According to Crowninshield and Brand (1981), this is achieved by minimising the non-linear objective function

$$\text{OBJ} = \sum \left(\frac{F_i}{\text{PCSA}_i} \right)^n, \qquad (15)$$

with n between 2.0 and 4.0, and where F_i represents the force exerted by muscle i, and PCSA_i its physiological cross-sectional area. In this case, $n = 2$ has been used.

This function is minimised and subjected to Eq. (14) together with the force balances of the tendon nets. Additional constraints to the problem are that tendon forces must be non-negative, and the limits of muscle forces obtained from Eqs. (3) and (4) when the muscle activation level is varied from 0 to 1

$$F_{\text{PEE}} F_{\max} \leqslant F \leqslant (F_l F_v + F_{\text{PEE}}) F_{\max}. \qquad (16)$$

The MATLAB system and its optimisation toolbox (version 5.2) have been used to implement the model.

2.2. Simulations

Free flexion–extension movements of the index finger and free MCP adduction motion have been simulated in order to validate the model. The muscle activation levels estimated by the model for these movements have been compared with the EMG data reported in literature to discuss its validity. To perform the simulations, posture data as a function of time during these actions have been measured and input to the model.

2.2.1. Free flexion–extension movements

Free flexion–extension movements of all index finger joints have been simulated based on posture data measured by the authors over one subject. The movement of the index finger during this action is basically a planar movement resulting from the combination of flexion–extension motion of the different joints, although some adduction of the MCP joint occurs during the extension phase. Under this consideration, a high-speed camera (Speedcam+) has been used to register the movement of the finger, being careful of placing the camera perpendicular to the motion plane. Acquisition speed of the camera was 100 Hz and the spacial resolution of the images 0.1 mm.

The subject was asked to perform flexion–extension movements of the index finger repeatedly. During the measurement, the subject kept his forearm and wrist resting on a horizontal surface with the wrist in neutral position of radioulnar deviation. All fingers are flexed and relaxed resting on the surface with the exception of the index finger, which performs cyclically the movements.

To measure the posture, two markers (0.5 mm $\times$ 0.5 mm) per segment have been used. The markers are aligned with the longitudinal axis of the segments so that the flexion angle corresponds to the angle between the straight lines connecting the points on each of the consecutive segments.

The approximate duration of each cycle was 0.4 s. The angle of the palm with the horizontal plane was 24°. The joint angles for all joints measured for one cycle and the angular velocities and accelerations calculated by numerically derivating the angles with respect to time are shown in Fig. 6. The cycle starts by extending the finger from flexed posture, achieves the full extension posture and then returns to the initial posture. A high correlation between the flexion angles of the PIP and DIP joints has been observed (0.968). The correlation between the flexion angles of MCP and PIP joints (0.929) is also high.

This action has been simulated using the model both with and without consideration of the inertial effects by entering zero angular velocities and accelerations, and with and without consideration of the passive forces generated by the muscles in order to analyse the importance of both factors over the model estimations.

2.2.2. Free adduction motion

To study the muscular behaviour during free abduction–adduction movements, the action of clockwise

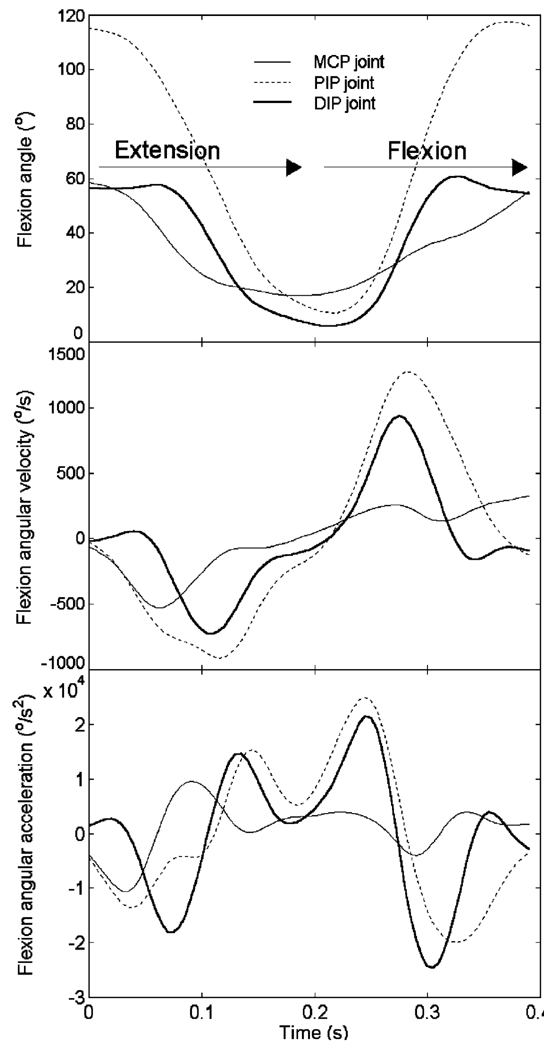

Fig. 6. Flexion angles and angular velocities and accelerations during the free flexion–extension movement.

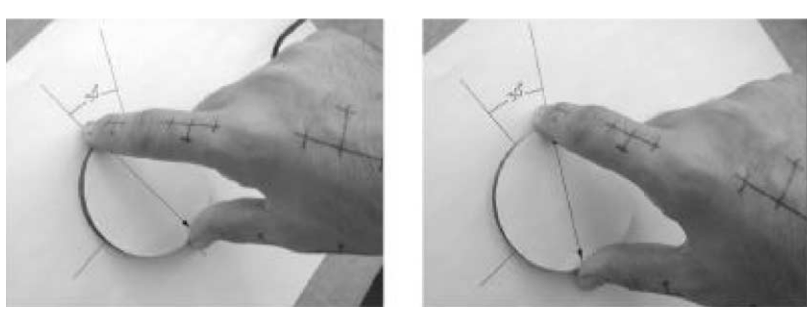

Fig. 7. Initial and final postures of the clockwise rotation simulated.

rotation of a disc 30° with the index finger and thumb has been simulated. No external force over the finger was considered except gravity (Fig. 7). Initial and final postures of the movement were measured using a photogrametric technique developed by the authors (Vergara-Monedero et al., 1999). No significant motion of the wrist was observed during the movement. Angles, angular velocities and angular accelerations defining the movement have been estimated from these postures considering an angle change pattern as in Brook et al. (1995). The values considered for the angles and angular velocities for each joint are presented in Fig. 8. The wrist is considered to be in neutral position of flexion and lateral deviation, and the forearm flexed so that the angle of the palm of the hand with the horizontal plane is 40°.

This action has been simulated both with and without consideration of the action of the ligaments in order to analyse its importance over the model estimations.

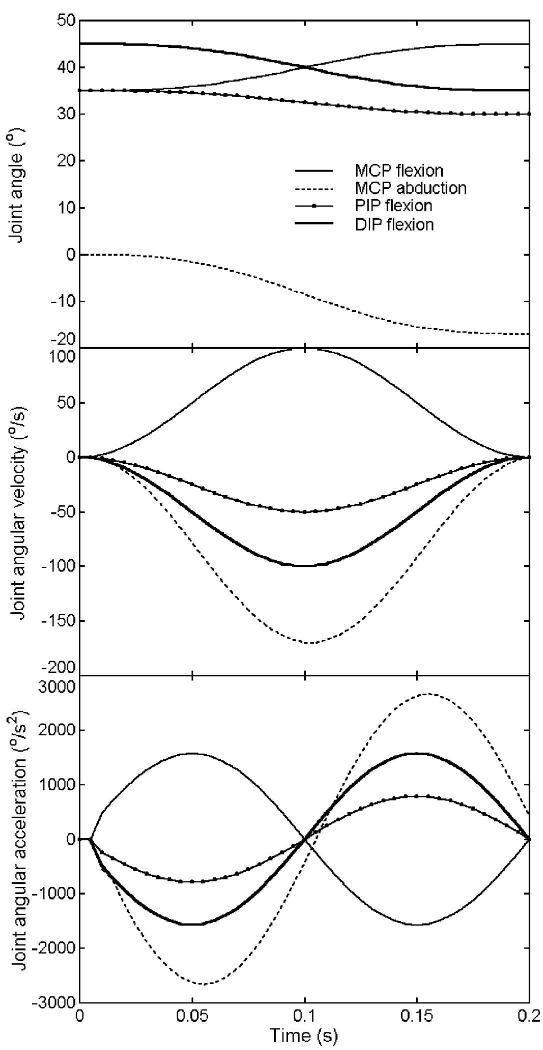

Fig. 8. Joint angles and joint angular velocities and accelerations during the free adduction motion.

3. Results and discussion

3.1. Results from free flexion–extension movements simulation

The estimated values of tendon excursions calculated with the biomechanical model during the simulation are within the range of excursions reported by An et al. (1983) (Fig. 9a). Positive values correspond to a length increment of the tendon path over the finger from the reference posture. Flexor tendon excursions decrease during the finger flexion, while extensor tendon excursions increase.

In order to analyse the muscular efforts estimated with the model, two phases have been considered: free extension movement and free flexion movement. Muscle action will vary depending on the phase being analysed.

As it was expected, extensor muscles participate actively during the free extension phase of the joints (Fig. 9b). At the beginning of this phase, the finger is flexed, and the flexor muscles are not stretched. Under these circumstances the extensor activity decreases as the acceleration required to extend the joint decreases. But when finger posture becomes more extended, extensor activity increases again because of the passive force exerted by the lengthened flexor muscles. The force exerted by the extensors increases considerably during the final period of the free flexion movement, corresponding to the deceleration of the flexion movement. This result agrees with the electromyographic (EMG) data from Darling et al. (1994) and Landsmeer and Long (1965), who first postulated the behaviour of the extensor as a brake during the free flexion movement of finger joints. If no inertial effects are considered, the model cannot reproduce the extensor activity during the flexion deceleration phase nor the extension acceleration phase (Fig. 10a). If no passive forces of the muscles are considered, the model does not estimate any significant activity for the extensors during full extension phase (Fig. 10b).

In accordance with the work of Long (1968), the model does not estimate any activity for the FDS during the free extension-flexion movement of the index finger (Fig. 9c). No activation of the FDP has been estimated during the deceleration phase of the free extension movement. According to the observations of Darling et al. (1994), the braking of the motion in this case primarily resulted from passive forces (lengthened extrinsic flexors). The model predicts that the force required to drive the free flexion motion is provided by the passive force exerted by the lengthened flexor muscles at the beginning of this phase, gravity and an active force generated by the FDP, according to the observations of Darling et al. (1994).

A similar pattern for the RI and EDC activities is observed (Fig. 9d) according to the observations

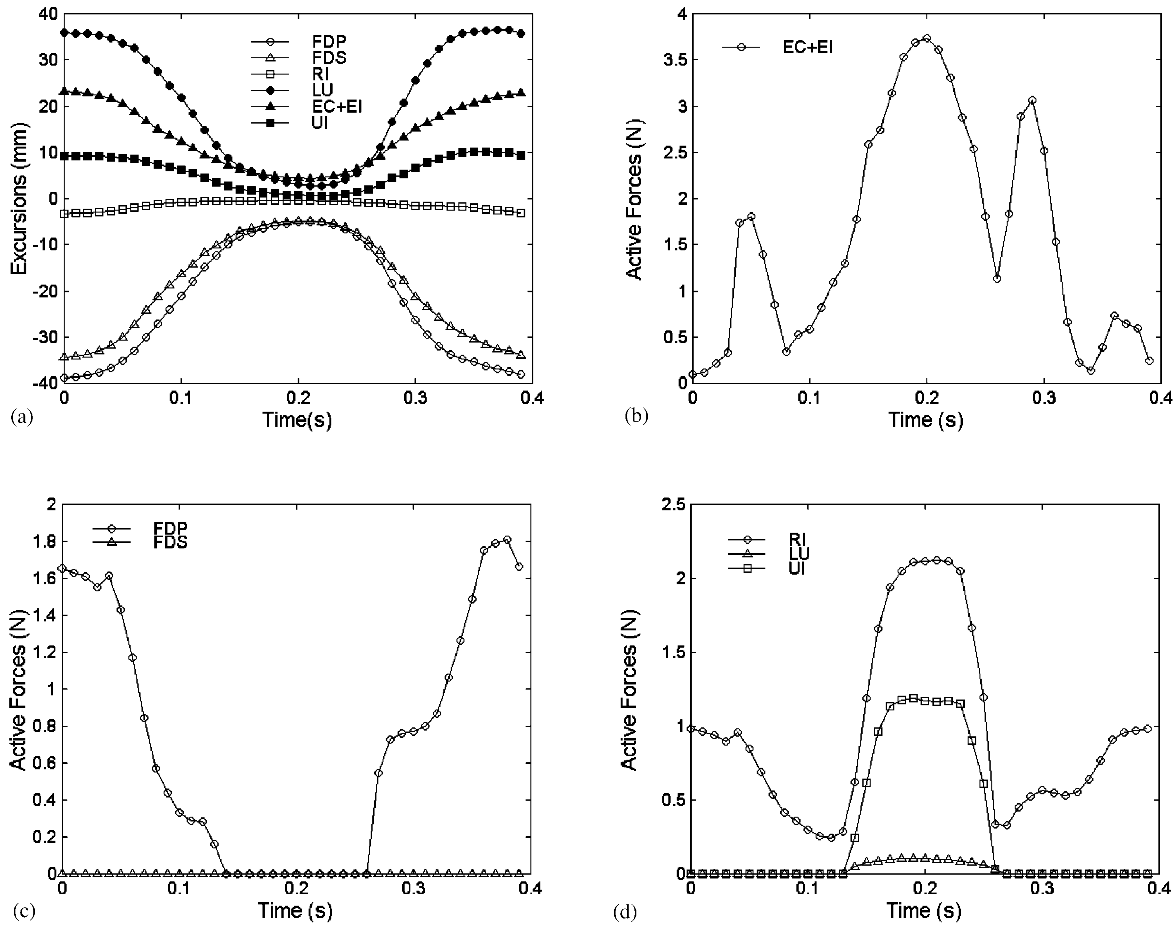

Fig. 9. Results from free flexion–extension motion simulation: (a) excursions estimated by the model; (b) Active forces estimated for the extrinsic extensor muscles; (c) active forces estimated for the extrinsic flexor muscles; (d) active forces estimated for the intrinsic muscles.

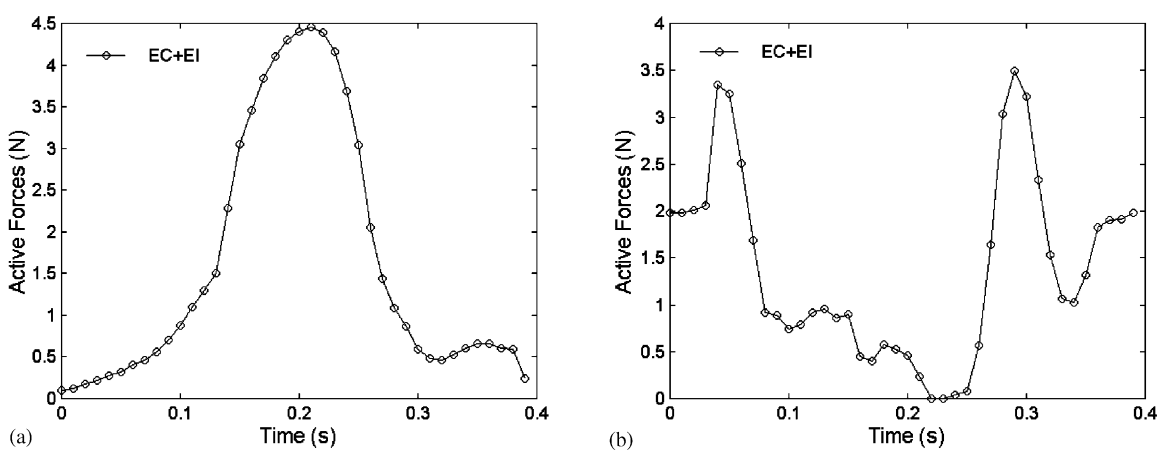

Fig. 10. Active forces estimated for the extrinsic extensor muscles during free flexion–extension motion simulation when: (a) no inertial effects are considered; (b) no passive forces exerted by the muscles are considered.

of Darling et al. (1994). The UI muscle participates actively in full extension, because of its contribution to the extensor mechanism. An active participation for the LU muscle during all the free extension phase was expected according to the works of Long et al. (1970) and Darling et al. (1994). However, the model only predicts activation for LU muscle near full extension.

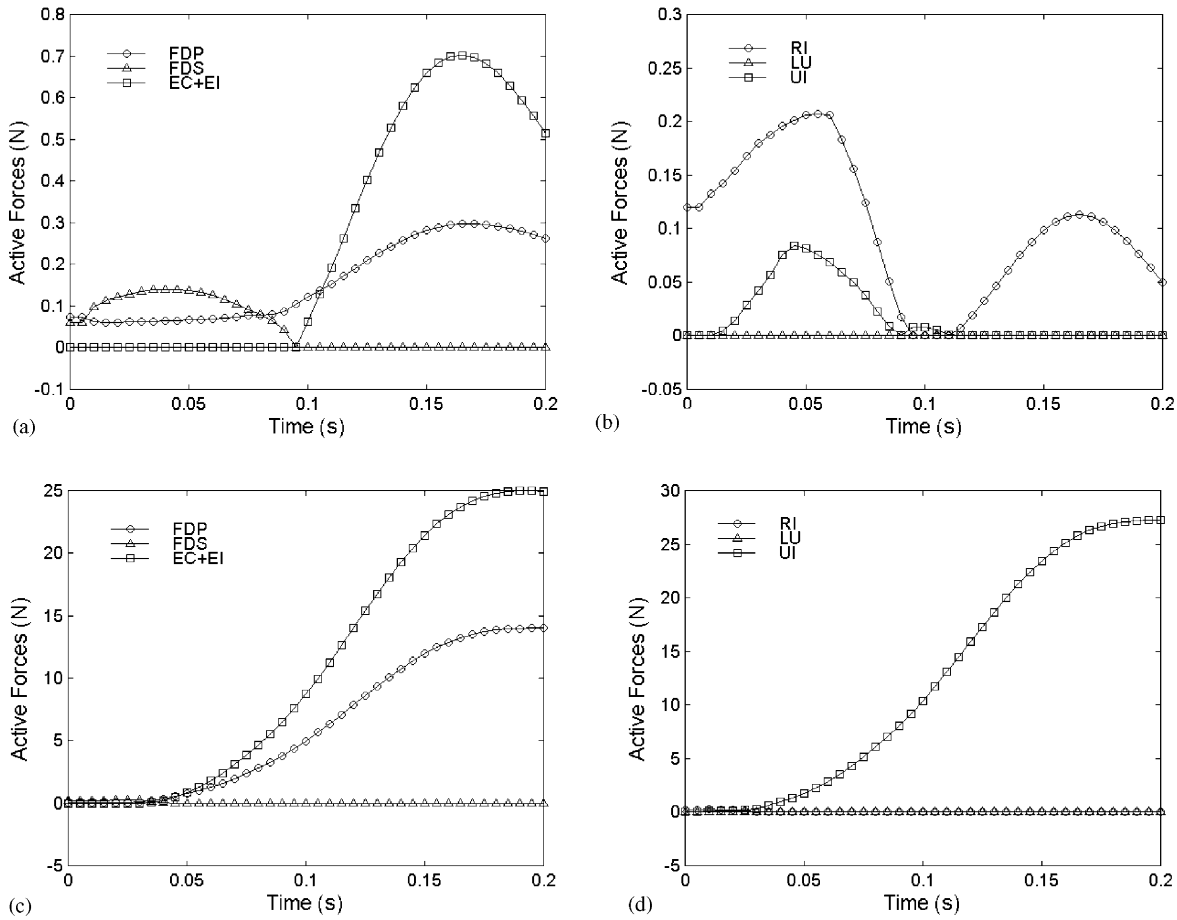

Fig. 11. Results from free abduction motion simulation: (a) active forces estimated for the extrinsic muscles without considering ligaments; (b) active forces estimated for the intrinsic muscles without considering ligaments; (a) active forces estimated for the extrinsic muscles considering ligaments; (b) active forces estimated for the intrinsic muscles considering ligaments.

3.2. Results from free adduction motion simulation

The model has been used to estimate active forces for the extrinsic and intrinsic muscles of the index finger when no ligaments are considered (Figs. 11a and 11b). No activation of the UI during the final phase of the adduction motion is estimated, and only a slight activation during the initial phase is predicted. The adduction moment generated by the weight of the phalanxes is enough to counteract the passive forces of the lengthened RI and to produce the adduction motion. This result does not agree with the EMG data reported by Long et al. (1970), who observed that the UI is the most active muscle during these movements. The results are quite different if the ligaments are considered (Figs. 11c and 11d). As the adduction increases, the radial collateral ligament becomes taut, and therefore, the UI muscle has to increase its activity to counteract the passive abduction moment generated by the ligament. The UI muscle produces an excess of flexion moment over the MCP joint to drive the flexion motion required. This excess is balanced by the EDC action, according to the observations from Long et al. (1970) (Fig. 11c).

4. Conclusions

A 3D dynamic model of the finger has been proposed based on its functional anatomic description. The validity of the model to estimate muscle forces involved during free movements has been proved by means of two simulations. The results from the free flexion–extension movements simulation have shown the importance of considering the inertial effects when estimating the muscular behaviour during fast movements, such as the work of the extensor muscles acting as a brake of the flexion movement. They have also pointed out the relevance of modelling the passive forces generated by the structures when studying free movements, such as the force exerted by the muscles when they are stretched, effects that cannot be neglected under these circumstances. The results from the free MCP adduction motion simulation have revealed the importance of considering the passive action of the ligaments over the MCP joint in order to reproduce the muscular force pattern during the simulation of the free MCP abduction–adduction movements.

Acknowledgements

We thank the *National Hansen's Disease Programs* and the support of the *Fundació Bancaixa* and the *Universitat Jaume I* for the project Ref. P1A97-06, in which this work is partially included.

References

An, K.N., Chao, E.Y.S., Kaufman, K.R., 1991. Analysis of muscle and joint loads. In: Mow, V.C., Hayes, W.C. (Eds.), Basic Orthopaedics Biomechanics. Raven Press Ltd., New York, pp. 1–50.

An, K.N., Cooney, W.P., 1991. Biomechanics of the hand. In: Morrey, B.F. (Ed.), Joint Replacement Arthroplasty. Churchill Livigstone, New York.

An, K.N., Ueba, Y., Chao, E.Y.S., Cooney, W.P., Linscheid, R.L., 1983. Tendon excursion and moment arm of index finger muscles. Journal of Biomechanics 16 (6), 419–425.

Biryukova, E.V., Yourovskaya, V.Z., 1994. A model of human hand dynamics. In: Schuind, F., An, K.N., Cooney III, W.P., Garcia-Elias, M. (Eds.), Advances in the Biomechanics of the Hand and Wrist. Plenum Press, New York, pp. 107–122.

Casolo, F., Lorenzi, V., 1994. Finger mathematical modelling and rehabilitation. In: Schuind, F., An, K.N., Cooney III, W.P., Garcia-Elias, M. (Eds.), Advances in the Biomechanics of the Hand and Wrist. Plenum Press, New York, pp. 197–223.

Chao, E.Y., An, K.N., 1978. Graphical interpretation of the solution to the redundant problem in biomechanics. Journal of Biomechanical Engineering 100, 159–167.

Chao, E.Y., Opgrande, J.D., Axmear, F.E., 1976. Three dimensional force analysis of finger joints in selectec isometric hand functions. Journal of Biomechanics 9, 387–395.

Craig, S.M., 1992. Anatomy of the joints of the fingers. Hand Clinics 8 (4), 693–700.

Crowninshield, R.D., Brand, R.A., 1981. A physiologically based criterion of muscle force prediction in locomotion. Journal of Biomechanics 14, 793–801.

Darling, W.G., Cole, K.J., Miller, G.F., 1994. Coordination of index finger movements. Journal of Biomechanics 12, 479–491.

Dubousset, J.F., 1981. The digital joints. In: Tubiana, R. (Ed.), The Hand. Saunders Company, Philadelphia, pp. 191–201.

Esteki, A., Mansour, J.M., 1997. A dynamic model of the hand with application in functional neuromuscular stimulation. Annals of Biomedical Engineering 25, 440–451.

García de Jalón, J., Bayo, E., 1994. Kinematic and dynamic simulation of multibody systems. Springer, New York.

Hatze, H., 1981. Myocibernetic Control Models of Skeletal Muscle. University of South Africa, Pretoria.

Kapandji, A.I., 1998. Fisiologie articulaire. Membre Supérieur. Editions Maloine, Paris.

Kaufman, K.R., An, K.N., Litchy, W.J., Chao, E.Y.S., 1991. Physiological prediction of muscle forces I. Theoretical formulation. Journal of Neuroscience 40 (3), 781–792.

Landsmeer, J.M.F., Long, C., 1965. The mechanism of finger control, based on electromyograms and location analysis. Acta Anatomica 60, 330–347.

Lee, J.W., Rim, K., 1990. Maximum finger force prediction using a planar simulation of the middle finger. Proceedings of the Institution of Mechanical Engineers. Part H. Journal of Engineering in Medicine 204, 169–178.

Long, C., 1968. Intrinsic–extrinsic muscle control of the fingers. Journal of Bone and Joint Surgery 52A, 973–984.

Long, C., Conrad, P.W., Hall, E.A., Furler, S.L., 1970. Intrinsic–extrinsic muscle control of the hand in power grip and precision handling. The Journal of Bone and Joint Surgery 52A (5), 853–867.

Mansour, J.M., Rouvas, C., Sarangapani, J., Hendrix, L., Crago, P.E., 1994. Quantitative functional anatomy of finger muscles: application to controlled grasp. In: Schuind, F., An, K.N., Cooney III, W.P., Garcia-Elias, M. (Eds.), Advances in the Biomechanics of the Hand and Wrist. Plenum Press, New York, pp. 177–188.

Minami, A., An, K.N., Cooney, W.P., Linscheid, R.L., 1985. Ligament stability of the MCP joint: a biomechanical study. Journal of Hand Surgery 10A (2), 255–260.

Mommersteeg, T.J.A., Blankevoort, L., Huiskes, R., Kooloos, J.G.M., Kauer, J.M.G., 1996. Characterization of the mechanical behavior of human knee ligaments: a numerical-experimental approach. Journal of Biomechanics 29 (2), 151–160.

Valero-Cuevas, F.J., Zajac, F.E., Burgar, C.G., 1998. Large index-fingertip forces are produced by subject-independent patterns of muscle excitation. Journal of Biomechanics 31, 693–703.

Vergara-Monedero, M., Sancho-Bru, X., Pérez-González, A., 1999. Measuring the hand posture from digital photographic images. Application to the study of the tip-pinch precision grip. In Proceedings of the 11th ADM International Conference on Design Tools and Methods in Industrial Engineering. Palermo.

Youm, Y., Gillespie, T.T, Flatt, A.E., Sprague, B.L., 1978. Kinematic investigation of normal MCP joint. Journal of Biomechanics 11, 109–118.

Zajac, F.E., 1989. Muscle and tendon: properties, models, scaling, and application to biomechanics and motor control. Critical Reviews in Biomedical Engineering 17 (4), 359–411.